Journal of Porphyrins and Phthalocyanines
*J. Porphyrins Phthalocyanines* 2015; **19**: 1–7
DOI: 10.1142/S1088424615500789

*Published at http://www.worldscinet.com/jpp/*

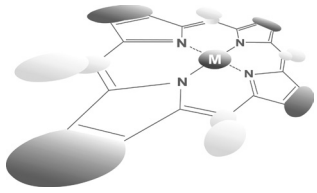

# Water-soluble porphyrin-phosphonate conjugates as potential photodynamic therapy photosensitizers

**Yunguo Lu[a‡], Zhihang Chen[b‡], Bingqiong Yu[a], Kun Yan*[a] and Zaoying Li*[a]**

[a] *College of Chemistry and Molecular Sciences, Wuhan University, Wuhan 430072, P.R. China*
[b] *Department of Radiology, Johns Hopkins University School of Medicine, Baltimore, Maryland 21287, USA*

*Received 14 April 2015*
*Accepted 22 June 2015*



**ABSTRACT:** Two novel water-soluble porphyrin-phosphonate conjugates were synthesized and characterized. Although both conjugates showed significant potential in photodynamic therapy, the variety of their structure induced the obvious differences in the binding manner with calf thymus DNA, the cytotoxicity and the cellular sublocalization.

**KEYWORDS:** porphyrin-phosphonate conjugates, photodynamic therapy, photosensitizers, DNA.

## INTRODUCTION

Photodynamic therapy (PDT) has been emerging as an effective modality for the selective treatment of cancers and other diseases for many years [1, 2]. Due to the non-targeted distributions of the photosensitizers (PSs), which lead to unwanted photodynamic effects in normal tissues [3], PDT has been mostly limited to cure melanomas and solid tumors like the bladder and the esophagus [4], which occurred in externally accessible cavities. To overcome these limitations, especially the undesirable side-effects, PSs have been conjugated with some biological molecules, such as carbohydrates [5, 6], monoclonal antibodies [7, 8], peptides [9–11], oligo-nucleotides [12] and some other natural products [13], to improve their biocompatibility, selectivity, efficacy and stability.

The porphyrin tend to accumulate in neoplastic tissue to higher concentrations than in surrounding normal tissue, and they might be photo-triggered to produce singlet-state oxygen to cleave DNA and eventually damage the tumor cells [14]. Therefore, porphyrin compounds have attracted significant attention in cancer diagnosis and treatment using photodynamic therapy(PDT) [15, 16].

Phosphonate, which is an important component of cell membranes and nucleotides, widely exists in the human body. Meanwhile, its derivates have a variety of therapeutic benefits. Inositol-phosphonates analogs have been reported to show good inhibition to non-small cell lung cancer (NSCLC) cell growth together with less toxicity against normal breast epithelial cell (MCF10A) [17]; anthracene-phosphonate conjugate (TEABP) was indicated as a selective anticancer agent in apoptosis mediated cancer therapy for U937 cell [18]; phosphonate-functionalized nanoparticles provided a promising basis for further development of biodegradable nanoparticles with high intracellular uptake rates or for drug release in a specific target cell [19].

Here we designed and synthesized two novel water-soluble cationic porphyrin-phosphonate conjugates (Chart 1), as potential photodynamic agents with high therapy efficiency and biocompatibility.

## RESULTS AND DISCUSSION

### Preparation of porphyrin-phosphonate conjugates

The water-soluble porphyrin **P1**, which was used as the control compound in our bioactivity studies, was synthesized as described in the literature [20]. The syntheses of porphyrin-phosphonate conjugates **P2** and **P3** were carried out as shown in Scheme 1. In brief, compound **1**, which was prepared as described in the literature, was transfered to compound **2** with active hydroxyl by boron tribromide. Then diethyl phosphorochloridate and

*Correspondence to: Kun Yan, email: kyan@whu.edu.cn; Zaoying Li, email: zyliwuc@whu.edu.cn, tel: + 86 27-68752366, fax: + 86 27-68754067

‡Equally contributing authors

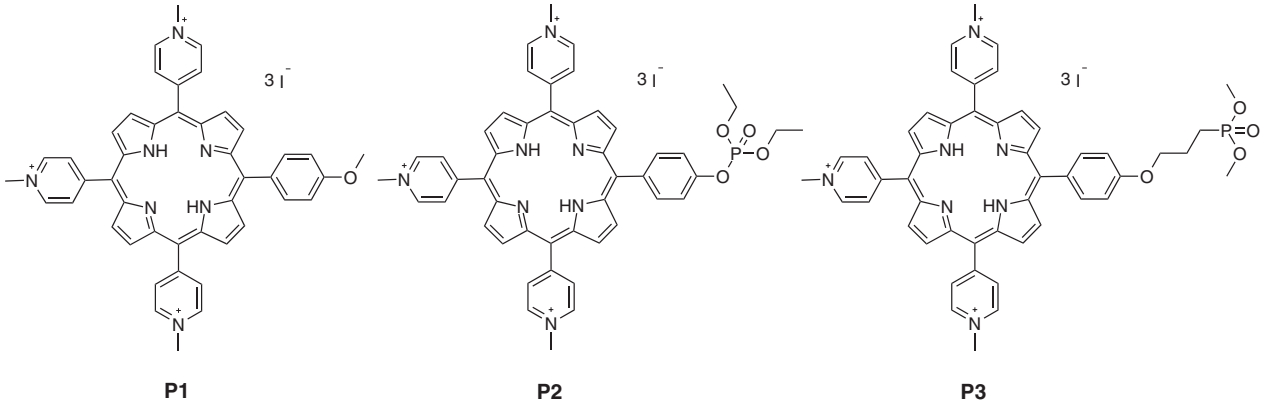


**Chart 1.** Molecular structure of **P1**–**P3**



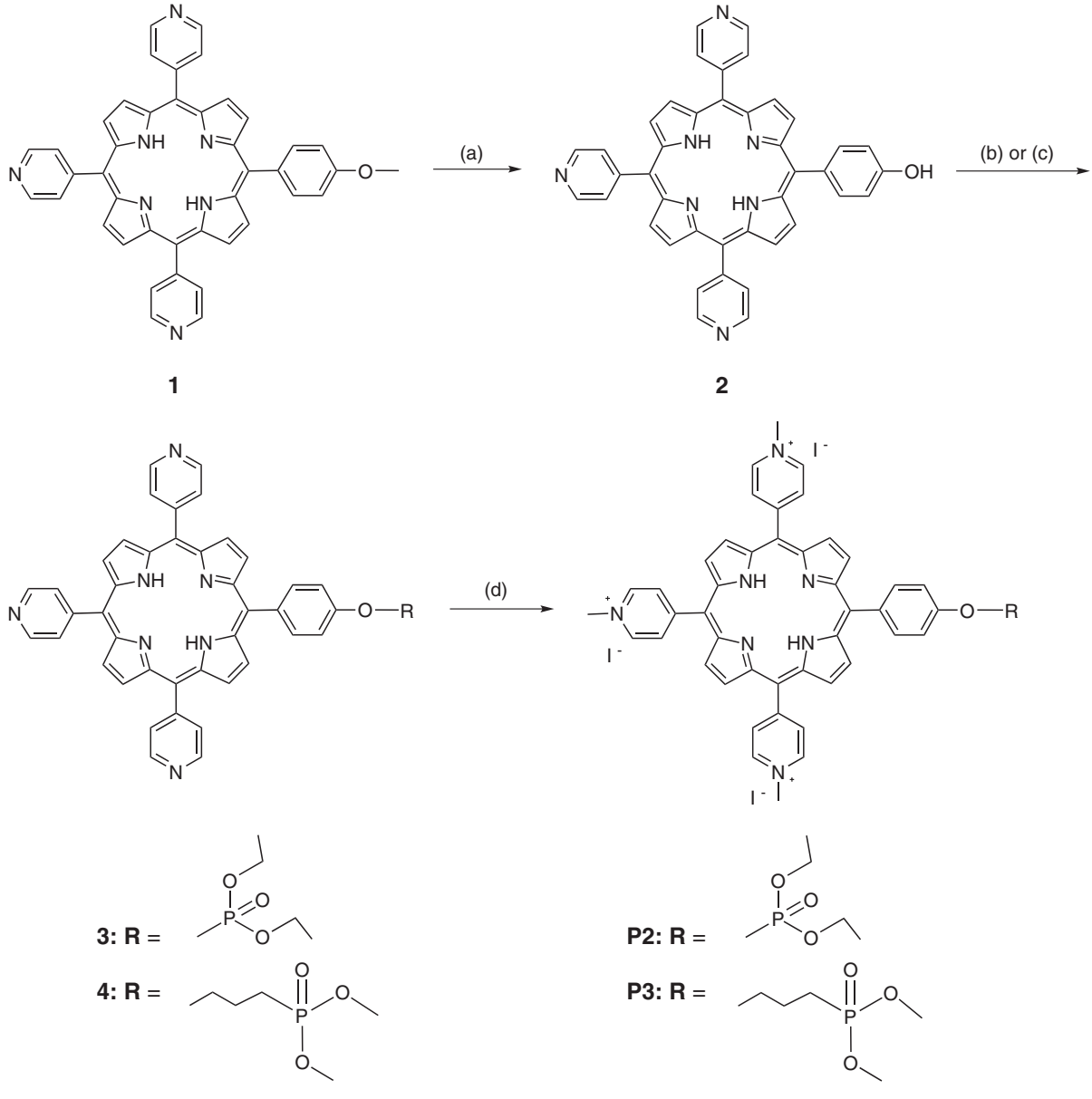


**Scheme 1.** Preparation of water-soluble porphyrin-phosphonate conjugates. Reagents and conditions: (a) $BBr_3$, $CH_2Cl_2$, 0 °C to rt, overnight; (b) $ClPO(OC_2H_5)_2$, $K_2CO_3$, DMF, 70 °C, 8 h; (c) $BrCH_2CH_2CH_2PO(OCH_3)_2$, $K_2CO_3$, DMF, 70 °C, 8 h; (d) $CH_3I$, DMF, rt, overnight

dimethyl(3-bromopropyl)phosphonate [21, 22] coupled with compound **2** in the presence of $K_2CO_3$ respectively to afford porphyrin **3** and **4** in good yields. Finally, the *N*-methylation of pyridine in porphyrin rings with excess of methyl iodide in DMF resulted in desired cationic conjugate **P2** or **P3** in high yields.

### *In vitro* photocytotoxicity

The photocytotoxicities of **P1**–**P3** against human prostate cancer cell line PC3 and human breast cancer cell line MDA-MB-231 were determined by the MTT assay. The cells were incubated with medicines in dark for 12 h, then replenished with fresh medium and irradiated with lights (10 J/cm$^2$) by mercury lamp. After another 24 h incubation in dark, cell viabilities are determined. The cell viabilities are listed in Table 1, in which the cytotoxicities were expressed as the drug concentration that inhibits cell proliferation by 50% ($IC_{50}$). As seen in Table 1, all porphyrins were considered to be nontoxic in the dark as the values of $IC_{50}$ were larger than 100 μM. With light irradiation, **P1** and **P3** exhibited similar significant cytotoxicity against the cancer cells in the nanomolar range. It is noteworthy that **P2** had 6-fold less cytotoxic effect than **P1** and **P3**.

### Spectroscopic properties

The interaction of cationic porphyrins **P1**–**P3** with calf thymus DNA (CT DNA) was studied by UV-vis spectrum, fluorescence titration and CD spectrum (Figs 1–3). The spectral measurements were performed at 25 °C in buffer solution (50 mM Tris-HCl, 100 mM NaCl, pH = 7.4). The UV-vis absorption spectra of **P1**–**P3** (3.0 μM) with addition of CT DNA are shown in Fig. 1. With increasing amounts of CT DNA (0–3.2 μM), the absorption spectra of **P1** and **P3** showed the red shift of 10–11 nm and the hypochromicities of 40–42%. However, further addition of CT DNA (3.5–50.0 μM) led to the additional red shift of 3–5 nm and the unexpected hyperchromicities of about 5%, which indicated that the binding model towards CT DNA might have been changed from an intercalative binding to a mixed binding model [23]. However, there was no similar inflection point in the titration spectra of **P2**, and the absorption spectra of **P2** only showed a red shift of 7 nm and a lower hypochromicity of 35%. The lack of hyperchromicity at high DNA/**P2** ratio indicates that binding manner of **P2** to DNA is different from the binding manner of **P1** and **P3** to DNA, and the sterical effect [24] is the main possible reason that causes this difference.

The results of fluorescence titration with CT DNA for **P1**–**P3** are shown in Fig. 2. The emission spectra of cationic porphyrin conjugate **P1**–**P3** (3.0 μM) were recorded with increasing amounts of CT DNA (0–50 μM). The fluorescence intensities of **P1**–**P3** all displayed significant decreases around 665 nm with the addition of CT DNA, indicating they adopt an outside binding or a combination of intercalation and outside binding mode

**Table 1.** Cytotoxicities ($IC_{50}$, μM) of **P1**–**P3** against PC3 and MDA-MB-231 cells (irradiation energy: 10 J/cm$^2$)

| Porphyrins | PC3 | | MDA-MB-231 | |
|---|---|---|---|---|
| | In dark | With light irradiation | In dark | With light irradiation |
| **P1** | >100 | 0.24 ± 0.004 | >100 | 0.30 ± 0.004 |
| **P2** | >100 | 1.42 ± 0.005 | >100 | 2.06 ± 0.003 |
| **P3** | >100 | 0.25 ± 0.004 | >100 | 0.31 ± 0.005 |

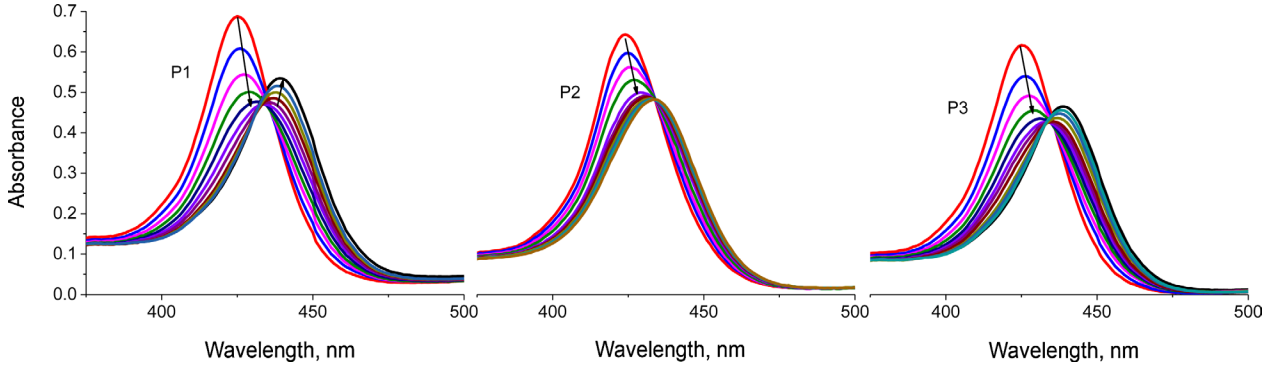


**Fig. 1.** Absorbance spectra of **P1**–**P3** (the concentrations of porphyrin are 3.0 μM, arrows indicate the change in intensity with increasing of CT DNA concentrations)

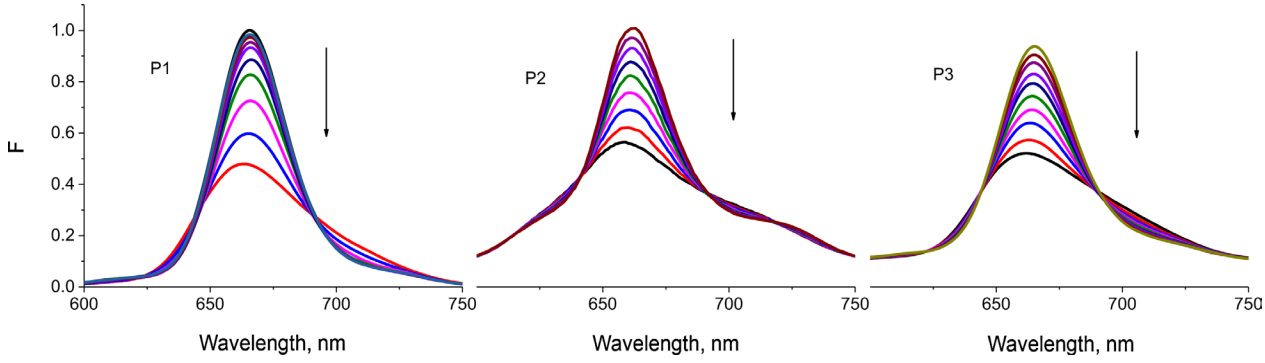


**Fig. 2.** Fluorescence spectra of **P1**–**P3** (the concentrations of porphyrin are 3.0 μM, arrows indicate the change in intensity with increasing of CT DNA concentrations)

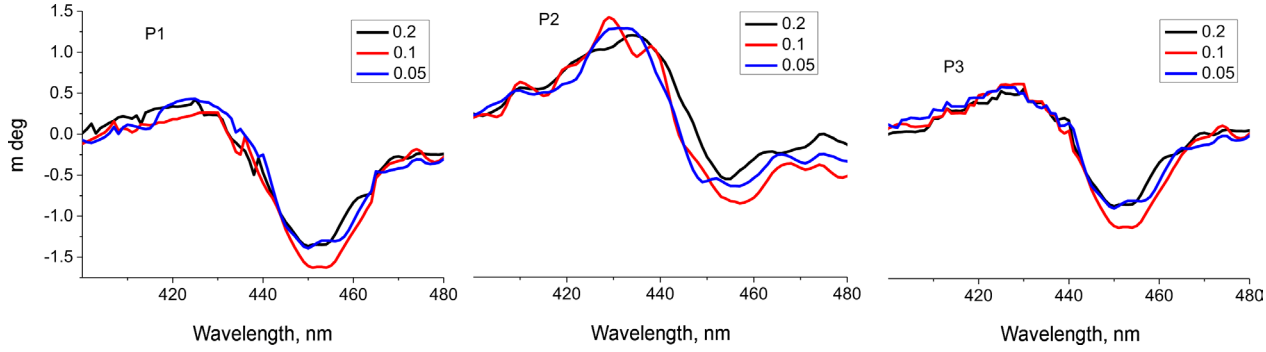


**Fig. 3.** Induced CD spectra of **P1**–**P3** (the concentrations of porphyrin are 10.0 μM, the ratio of [porphyrin]/[DNA base pair] running from 0.2 to 0.05)

with CT DNA. The binding constant ($K$, $M^{-1}$) values are $3.39 \times 10^5$, $3.18 \times 10^5$ and $3.71 \times 10^5$, respectively for **P1**, **P2** and **P3** [25].

To further clarify the binding mode, the induced CD spectra of the porphyrins were recorded in the presence of CT DNA. As shown in Fig. 3, the strong negative peaks of all conjugates centered at 452 nm indicated the intercalation mode. The weak positive peaks centered at 428 nm had appeared in the spectra of **P1** and **P3**. The strong positive peaks centered at 428 nm were observed in the spectra of **P2**, which revealed that outside binding also took a role in the interaction [26–28]. When porphyrin compounds interacted with CT DNA, intercalation was dominant for **P1** and **P3**, but outside binding was dominant for **P2** due to the steric effect.

### Subcellular localization

The confocal laser scan microscope was performed to investigate the cell up-takes and localization of **P1**–**P3** in PC3 cells and MDA-MB-231 cells. All of the imaging pictures were obtained with same instrument parameters and the results are shown in Fig. 4. In both PC3 and MDA-MB-231 cells, it is obvious that the fluorescence intensities of **P1** and **P3** were stronger than that of the **P2**. Because of the similar molar extinction and fluorescence quantum yields. It indicated the cell up-takes of **P1** and **P3** were higher than that of **P2**; therefore the higher cell up-takes were the possible main reason that causes the higher cytotoxicity of **P1** and **P3**. **P2** and **P3** both showed almost uniform distribution in the entire cell, and there was no obvious organelle specificity. Although the obvious enrichment of **P1** in cytoplasm could been seen, there was no significant organelle specificity of **P1** when compared with other organelle specifical probe such as mitochondrion, lysosome, Golgi, ER and endosome. Compared with **P2** and **P3**, **P1** without phosphonate had the higher positive charge density and smaller steric hindrance. Therefore we considered that **P1** was easy to bind and aggregated with protein in cytoplasm, and this stronger interactions with protein induced the non-specific enrichment of **P1** in cytoplasm.

## EXPERIMENTAL

### Material and methods

Pyrrole, 4-pyridinecarboxaldehyde, 4-methoxybenzaldehyde, 1,3-dibromopropane, trimethyl phosphite and triethyl phosphite were freshly redistilled before using. All reaction solvents were dried and purified according to standard procedures. The 5-(4-methoxyphenyl)-10,15,20-tri(pyridin-4-yl) porphyrin (**1**) was synthesized according

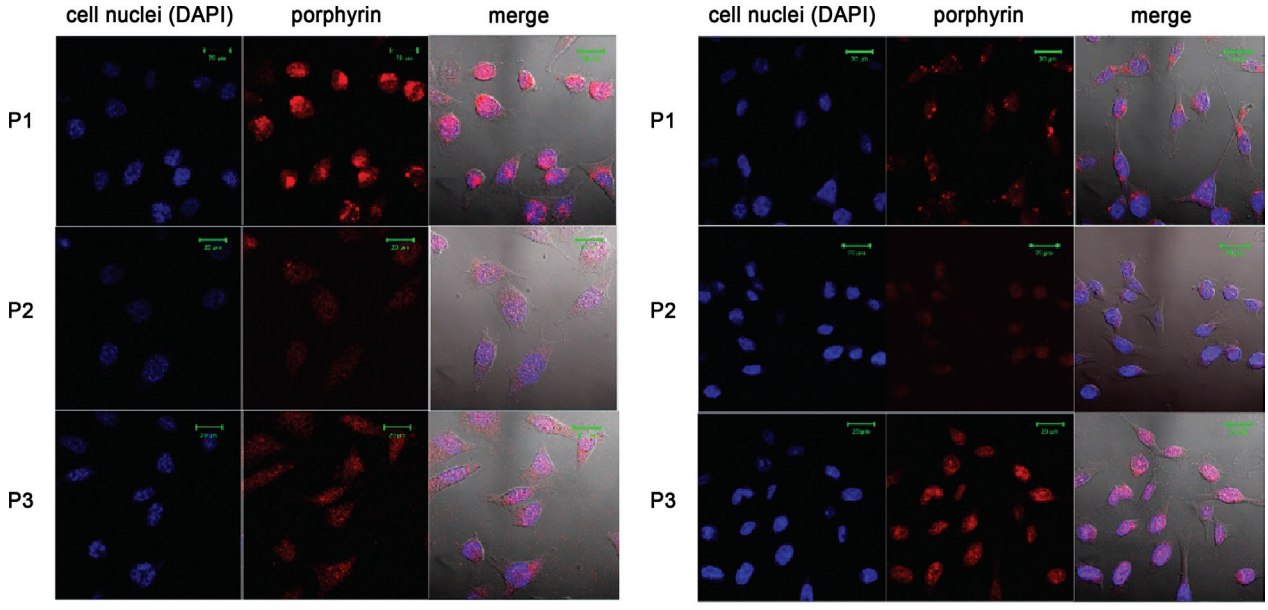


**Fig. 4.** Laser confocal fluorescence microscopy images of **P1**–**P3** in (left) PC3 cells and (right) MDA-MB-231 cells (dosage: 5 μM; incubation time: 6 h)



to literature method [20]. Diethyl phosphorochloridate was synthesized according to the literature [21], and dimethyl (3-bromopropyl)phosphonate was prepared following the literature [22]. UV-visible spectra were recorded on a Shimadzu 1601 spectrophotometer. Fluorescence spectra were recorded on PerkinElmer LS-55 fluorospectrophotometer. Proton NMR spectra were measured using a Varian Mercury VX 300 spectrometer. Elemental analysis was performed on VarioEL III. High resolution electrospray ionization (ESI) mass spectra were obtained on Voyager DE-STR.

## Syntheses

**5-(4-Hydroxyphenyl)-10,15,20-tri(4-pyridinyl) porphyrin (2).** The 5-(4-methoxyphenyl)-10,15,20-tri(pyridine-4-yl) porphyrin **1** (100.0 mg, 0.15 mmol) was dissolved in dried and degassed $CH_2Cl_2$ (25 mL). The solution was stirred at -10 °C and $BBr_3$ (0.7 mL, 0.75 mmol) in 5 mL of $CH_2Cl_2$ was slowly added over 1 h. The bluish-green reaction mixture was allowed to warm to room temperature and stirred overnight under nitrogen. The mixture was quenched with methanol (3 mL), cautiously poured into a mixture of ice and saturated aqueous solution of $NaHCO_3$ and stirred for further 30 min. The resulting solid was isolated by suction filtration, thoroughly washed with cold water and $CHCl_3$, and drying in vacuum afford product **2** as purple solid. Yield 85%. $^1$H NMR (300 MHz; DMSO-$d_6$): δ, ppm 9.05 (d, $J$ = 6.8 Hz, 6H), 8.78–8.93 (m, 8H), 8.14 (d, $J$ = 6.6 Hz, 6H), 8.13 (d, $J$ = 9.6 Hz, 2H), 7.32 (d, $J$ = 9.6 Hz, 2H), -2.75 (s, 2H). Anal. calcd. for $C_{41}H_{27}N_7O$: C, 77.71; H, 4.29; N, 15.47%. Found C, 77.68; H, 4.25; N, 15.41.

**5-(4-(Diethoxyl-phosphonoxy)phenyl)-10,15,20-tri(4-pyridinyl)porphyrin (3).** To a solution of **2** (400.0 mg, 0.062 mmol) and $ClPO(OC_2H_5)_2$ (51.0 mg, 0.30 mmol) in 10 mL carefully dried DMF was added $K_2CO_3$ (500.0 mg, 3.62 mmol), after stirring for 10 h at 80 °C, the mixture was cooled to ambient temperature and saturated brine (30 mL) was added. The mixture was kept at 0 °C overnight and purple solid was isolated by suction filtration, washing with saturated brine, and drying in vacuum. The product was then purified by silica gel column chromatography with chloroform and methanol (v/v, 50:1) as eluant. The second purple-red band was collected. The solvents were removed under reduced pressure, and the final products were obtained by recrystallization from chloroform-petroleum ether. Yield 42.0 mg (88%). $^1$H NMR (300 MHz; $CDCl_3$): δ, ppm 9.05 (d, $J$ = 3.0 Hz, 6H), 8.91 (d, $J$ = 6.0 Hz, 2H), 8.84 (d, $J$ = 6.0 Hz, 6H), 8.82 (d, $J$ = 3.0 Hz, 2H), 8.17 (d, $J$ = 6.0 Hz, 2H), 8.16 (d, $J$ = 3.0 Hz, 6H), 7.64 (d, $J$ = 6.0 Hz, 2H), 4.43 (m, 4H), 1.52 (t, $J$ = 6.0 Hz, 6H), -2.91 (s, 2H). $^{31}$P NMR ($CDCl_3$): δ, ppm -6.07. Anal. calcd. for $C_{45}H_{36}N_7O_4P$: C, 70.21; H, 4.71%; N, 12.74. Found C, 70.44; H, 4.55; N, 12.69.

**5-(4-(Dimethoxy-phosphoryl-propyl-oxo-lphenyl)-10,15,20-tri(4-pyridinyl)porphyrin (4).** Compound **4** was prepared from porphyrin **2** (40.0 mg, 0.062 mmol) and $Br(CH_2)_3PO(OCH_3)_2$ (70.0 mg, 0.30 mmol) according to the method described above. Yield 41.0 mg (84%). $^1$H NMR (300 MHz; $CDCl_3$): δ, ppm 9.06 (d, $J$ = 3.0 Hz, 6H), 8.96 (d, $J$ = 6.0 Hz, 2H), 8.85 (d, $J$ = 6.0 Hz, 6H), 8.17 (d, $J$ = 6.0 Hz, 2H), 8.03 (d, $J$ = 3.0 Hz, 6H), 7.60 (d, $J$ = 6.0 Hz, 2H), 4.37 (d, $J$ = 9.9 Hz, 2H), 3.86 (d, $J$ = 9.6 Hz, 6H), 2.25–2.29 (m, 2H), 1.30 (t, $J$ = 8.4 Hz,

2H), -2.87 (s, 2H). HRMS (MALDI-TOF): *m/z* 784.1451 (calcd. for $[M + H]^+$ 784.2800).

**(5-(4-Methoxyl-phenyl)-10,15,20-tri(4-*N*-methylpyridy)porphyrin triiodide (P1).** A mixture of porphyrin **1** and methyl iodide were stirred at room temperature in dry DMF overnight. Then the solvent and the excess of methyl iodide were removed under vacuum. The residue was dissolved in DMF and precipitated with $CHCl_3$ to yield the cationic porphyrin **P1** in quantitative yields. $^1$H NMR (400 MHz; DMSO-$d_6$): δ, ppm 9.07 (d, $J$ = 7.0 Hz, 6H), 8.81–8.92 (m, 8H), 8.16 (d, $J$ = 7.0 Hz, 6H), 8.10 (d, $J$ = 10.0 Hz, 2H), 7.30 (d, $J$ = 10.0 Hz, 2H), 4.86 (s, 9H), 4.11 (s, 3H), -2.78 (s, 2H). UV-vis ($H_2O$): $\lambda_{max}$, nm (ε) 425 (135000); 520 (7390); 562 (4000); 585 (3760).

**5-(4-(Diethoxyl-phosphonoxy)phenyl)-10,15,20-tri-(4-*N*-methylpyridy)porphyrin triiodide (P2).** Cationic porphyrin-phosphonate **P2** was synthesized from compound **3** according to the method described above. $^1$H NMR (300 MHz; DMSO-$d_6$): δ, ppm 9.48 (d, $J$ = 3.0 Hz, 6H), 9.16 (d, $J$ = 6.0 Hz, 4H), 9.06 (d, $J$ = 6.0 Hz, 4H), 8.97 (d, $J$ = 3.0 Hz, 6H), 8.10 (d, $J$ = 3.0 Hz, 2H), 7.64 (d, $J$ = 3.0 Hz, 2H), 4.73 (s, 9H), 4.01–4.11 (m, 4H), 1.25 (t, $J$ = 6.0 Hz, 6H), -2.91 (s, 2H). UV-vis ($H_2O$): $\lambda_{max}$, nm (ε) 425 (89100); 520 (5900); 560 (3820); 583 (2860). HRMS (MALDI-TOF): *m/z* 814.1415 (calcd. for $[M]^+$ 814.3300).

**5-(4-(Dimethoxy-phosphoryl-propyl-oxo-lphenyl)-10,15,20-tri(4-*N*-methylpyridy)porphyrin triiodide (P3).** Cationic porphyrin-phosphonate **P3** was synthesized from **4** according to the method described above. $^1$H NMR (300 MHz, DMSO-$d_6$): δ, ppm 9.48 (d, $J$ = 3.0 Hz, 6H), 9.18 (d, $J$ = 6.0 Hz, 4H), 9.08 (d, $J$ = 6.0 Hz, 4H), 8.96 (d, $J$ = 3.0 Hz, 6H), 8.14 (d, $J$ = 6.0 Hz, 2H), 7.43 (d, $J$ = 6.0 Hz, 2H), 4.72 (s, 9H), 4.35 (d, $J$ = 9.9 Hz, 2H), 3.72 (d, $J$ = 9.6 Hz, 6H), 3.58–5.62 (m, 2H), 2.12–2.15 (m, 2H), -2.87 (s, 2H). UV-vis ($H_2O$): $\lambda_{max}$, nm (ε) 425 (115000); 523 (10800); 560 (9390); 583 (9030). HRMS (MALDI-TOF): *m/z* 829.1630 (calcd. for $[M]^+$ 828.3400).

### UV-vis and fluorescence titration spectroscopy

Interactions between cationic porphyrins and calf thymus DNA (ct DNA) were tested by UV-vis spectrum and fluorescence spectrum. ct DNA (Invitrogen) was dissolved in a buffer (pH = 7.4, 50 mM Tris-HCl, 100 mM NaCl). Initially, visible absorption and fluorescence spectrum of each porphyrin-phosphonate conjugate was measured at a concentration of $3.0 \times 10^{-6}$ M. Then ct DNA was added to each compound [porphyrin]/[DNA base pair] ratio running from 3.0 to 0.2.

### Circular dichroism (CD) studies

The spectral bandwidth was 2 nm, and the cell length was 1 cm. ct DNA was added to the porphyrins ($1.0 \times 10^{-6}$ M), and after an incubation period of 15 min, the samples were scanned in the visible region. R value, ratio of concentration of the porphyrin to concentration of DNA, was running from 0.2 to 0.05. Baseline was corrected using the same buffer before scanning the samples. The spectra were recorded in 3 mM Tris–HCl, 6 mM NaCl (pH 7.4).

### Cell viability assays

Cell lines (PC3, human prostate cancer cell line; MDA-MB-231, human breast cancer cell line) were grown according to media component mixtures, designated by American Type Culture Collection in RPMI-1640 with 10% fetal calf serum in a 5% $CO_2$ humidity incubator at 37 °C. The cells were seeded in 96-well plate at a density of $4 \times 10^3$ and incubated for 24 h before treatment. The cells were incubated with medicines in dark for 12 h, then replenished with fresh medium and irradiated with lights (10 J/cm$^2$) by mercury lamp. After further 24 h incubation in dark, cell viabilities were determined by 3-(4,5-dimethylthiazol-2-yl)-2,5-diphenyltetrazolium bromide (MTT) reduction assay. Optical density (OD) of dissolved formazan crystal was measured using a 96-well plate reader (Tecan Infinit F200) at 570 and 690 nm.

### Subcellular localization by fluorescence microscopy

Cells were plated in a 4-wells chamber silde, and grown for 24 h. The cells were then incubated with 1 μM porphyrins in complete medium for another 6 h. Cells were washed with PBS three times, then were fixed with 5% formaldehyde PBS solution. DAPI was applied to stain the cell nuclei. The confocal laser fluorescence microscope Zeiss LSM 510 META (Carl Zeiss, Inc. Oberkochen, Germany) was used to image the cells at a resolution of 1024 × 1024 pixels. Porphyrin and DAPI fluorescence images were obtained using $\lambda_{ex}$ = 405 nm and $\lambda_{em}$ = 680 nm, and $\lambda_{ex}$ = 405 nm and $\lambda_{em}$ = 420–480 nm filter sets respectively.

## CONCLUSION

Two water-soluble porphyrin-phosphonate conjugates **P2** and **P3** were prepared. Amongst them, **P3** showed similar bioactivities compared with the control porphyrin **P1**. The spectroscopic studies (UV-vis and CD titrations) suggested that **P3** could intercalate into DNA, which resulted in higher cell up-takes and lower $IC_{50}$ values against PC3 and MDA-MB-231 cancer cells. On the contrary, the conjugate P2 preferred to outside binding due to the steric effect, which resulted in obvious differences in the cytotoxicity and the cellular sublocalization.

### Acknowledgements

The study was supported by National Natural Science Foundation (NNSF) of China (Grant No. 21401144) and Nature Science Foundation of Hubei Province, China (Grant No. 2013CFB236).

## REFERENCES


1. Detty MR, Gibson SL and Wagner SJ. *J. Med. Chem.* 2004; **47**: 3897–3915.
2. Schmitt F and Juillerat–Jeanneret L. *Anti Cancer Agents in Med. Chem.* 2012; **12**: 500–525.
3. Pereira PMR, Carvalho JJ, Silva S, Cavaleiro JAS, Schneider RJ, Fernandes R and Tome JPC. *Org. Biomol. Chem.* 2014; **12**: 1804–1811.
4. Agostinis P, Berg K, Cengel KA, Foster TH, Girotti AW, Gollnick SO, Hahn SM, Hamblin MR, Juzeniene A, Kessel D, Korbelik M, Moan J, Mroz P, Nowis D, Piette J, Wilson BC and Golab J. *CA Cancer J. Clin.* 2011; **61**: 250–281.
5. Borbas KE, Mroz P, Hamblin MR and Lindsey JS. *Bioconjugate Chem.* 2006; **17**: 638–653.
6. Wirth T. *Angew. Chem. Int. Ed.* 2005; **44**: 3656–3665.
7. Endo M, Shiroyama T, Fujitsuka M and Majima T. *J. Org. Chem.* 2005; **70**: 7468–7472.
8. Li J, Wei YL, Guo LM, Zhang CH, Jiao Y, Shuang SM and Dong C. *Talanta* 2008; **76**: 34–39.
9. Kralova J, Kejik Z, Briza T, Pouckova P, Kral A, Martasek P and Kral V. *J. Med. Chem.* 2010; **53**: 128–138.
10. Sibrian-Vazquez M, Jensen TJ and Vicente MGH. *J. Med. Chem.* 2008; **51**: 2915–2923.
11. Yuasa M, Oyaizu K, Horiuchi A, Ogata A, Hatsugai T, Yamaguchi A and Kawakami H. *Mol. Pharm.* 2004; **1**: 387–389.
12. Sol V, Chaleix V, Granet R and Krausz P. *Tetrahedron* 2008; **64**: 364–371.
13. Kumar D, Mishra BA, Shekar KPC, Kumar A, Akamatsu K, Kurihara R and Ito T. *Org. Biomol. Chem.* 2013; **11**: 6675–6679.
14. Giri U, Iqbal M and Athar M. *Carcinogenesis* 1996; **17**: 2023–2028.
15. Dougherty TJ, Gomer CJ, Henderson BW, Jori G, Kessel D, Korbelik M, Moan J and Peng Q. *J. Natl Cancer Inst.* 1998; **90**: 889–905.
16. Ali H and van Lier JE. *Chem. Rev*. 1999; **99**: 2379–2450.
17. Song FB, Zhang J, Cui QB, Wang T, Chen WB, Li LY and Xi Z. *Tetrahedron Lett.* 2012; **53**: 1102–1104.
18. Pramanik M, Chatterjee N, Das S, Das Saha K and Bhaumik A. *Chem. Commun.* 2013; **49**: 9461–9463.
19. Tautzenberger A, Lorenz S, Kreja L, Zeller A, Musyanovych A, Schrezenmeier H, Landfester K, Mailander V and Ignatius A. *Biomaterials* 2010; **31**: 2064–2071.
20. Gianferrara T, Giust D, Bratsos I and Alessio E. *Tetrahedron* 2007; **63**: 5006–5013.
21. Poshkus AC and Herweh JE. *J. Am. Chem. Soc.* 1957; **79**: 6127–6129.
22. Hewitt DG and Teese MW. *Aust. J. Chem*. 1984; **37**: 205–210.
23. Sari MA, Battioni JP, Dupre D, Mansuy D and Lepecq JB. *Biochemistry* 1990; **29**: 4205–4215.
24. Kubat P, Lang K, Kral V and Anzenbacher P. *J. Phys. Chem. B* 2002; **106**: 6784–6792.
25. LePecq JB and Paoletti C. *J. Mol. Biol.* 1967; **27**: 87–106.
26. Pasternack RF, Gibbs EJ and Villafranca JJ. *Biochemistry* 1983; **22**: 2406–2414.
27. Carvlin MJ, Mark E, Fiel R and Howard JC. *Nucleic Acids Res.* 1983; **11**: 6141–6154.
28. Carvlin MJ and Fiel RJ. *Nucleic Acids Res.* 1983; **11**: 6121–6139.